Appl. Math. Mech. -Engl. Ed., **33**(2), 195–210 (2012)
DOI 10.1007/s10483-012-1543-9

Applied Mathematics and Mechanics (English Edition)

Numerical investigation of Dufour and Soret effects on unsteady MHD natural convection flow past vertical plate embedded in non-Darcy porous medium*

M. Q. AL-ODAT[1,2], A. AL-GHAMDI[1]

(1. Mechanical Engineering Department, Faculty of Engineering, Umm Al-Qura University, Makkah, Kingdom of Saudi Arabia;
2. Mechanical Engineering Department, Al-Huson University College, Al-Balqa Applied University, Irbid, Jordan)

Abstract The Dufour and Soret effects on the unsteady two-dimensional magnetohydrodynamics (MHD) double-diffusive free convective flow of an electrically conducting fluid past a vertical plate embedded in a non-Darcy porous medium are investigated numerically. The governing non-linear dimensionless equations are solved by an implicit finite difference scheme of the Crank-Nicolson type with a tridiagonal matrix manipulation. The effects of various parameters entering into the problem on the unsteady dimensionless velocity, temperature, and concentration profiles are studied in detail. Furthermore, the time variation of the skin friction coefficient, the Nusselt number, and the Sherwood number is presented and analyzed. The results show that the unsteady velocity, temperature, and concentration profiles are substantially influenced by the Dufour and Soret effects. When the Dufour number increases or the Soret number decreases, both the skin friction and the Sherwood number decrease, while the Nusselt number increases. It is found that, when the magnetic parameter increases, the velocity and the temperature decrease in the boundary layer.

Key words double-diffusive free convection, non-Darcy model, magnetohydrodynamic (MHD), porous medium, Dufour effect, Soret effect, numerical solution

Chinese Library Classification O357
2010 Mathematics Subject Classification 65-XX, 76-XX, 80-XX, 76W05, 76S05

Nomenclature

B_0,	magnetic induction;	Gr_c,	modified solutal Grashof number;
C,	concentration;	Gr_t,	thermal Grashof number;
c_p,	specific heat at constant pressure;	k_e,	effective thermal conductivity of porous medium;
c_s,	concentration susceptibility;		
Da,	Darcy number;	K_p,	permeability of porous medium;
D_m,	coefficient of mass diffusivity;	K_t,	thermal diffusion ratio;
Du,	Dufour number;	M,	magnetic field parameter;
F,	Forchheimer coefficient;	Nu,	Nusselt number;
g,	gravitational acceleration;	Pr,	Prandtl number;

* Received May 20, 2011 / Revised Nov. 10, 2011
Corresponding author M. Q. AL-ODAT, Professor, Ph. D., E-mail: m_alodat@yahoo.com

Sc,	Schmidt number;	u, v,	velocity components in x- and y- directions, respectively;
Sh,	Sherwood number;		
Sr,	Soret number;	u_0,	velocity of plate;
T,	temperature;	X,	dimensionless spatial coordinate along plate;
t,	time;		
T_∞,	free stream temperature;	Y,	dimensionless spatial coordinate normal to plate;
T_m,	mean fluid temperature;		
T_w,	wall temperature;	x,	spatial coordinate along plate;
U, V,	dimensionless velocity components in X- and Y-directions, respectively;	y,	spatial coordinate normal to plate.

Greek symbols

α_e,	effective thermal diffusivity;	τ,	dimensionless time;
Γ,	Forchheimer parameter;	ν,	effective kinematic viscosity of fluid;
ρ,	fluid density;	σ,	electrical conductivity of fluid;
ϕ,	dimensionless concentration variable;	β_c,	concentration expansion coefficient;
θ,	dimensionless temperature variable;	β_t,	thermal expansion coefficient.

Subscripts

w,	conditions at wall;	∞,	free stream conditions.

1 Introduction

The double-diffusive free convective flow past the porous media has several important applications in engineering and geophysics such as the thermal energy storage and recovery system, the petroleum reservoir, the building insulation, the migration of moisture through the air contained in fibrous insulation, the geothermal energy extraction, the underground disposal of nuclear wastes, the spreading of chemical contaminants through water-saturated soil, and many others. A comprehensive review on this area was presented by Nield and Bejan[1] and Ingham and Pop[2].

The Dufour and Soret effects were neglected in many reported reasearch studies, since they are of a smaller order of magnitude than the effects described by Fourier's and Fick's laws. When the heat and mass transfer occurs simultaneously in a moving fluid, the relations between the fluxes and the driving potentials are more complicated. It was found that an energy flux can be generated not only by the temperature gradients but also by the composition gradients. The mass transfer caused by the temperature gradient is called the Soret effect, while the heat transfer caused by the concentration gradient is called the Dufour effect. However, such effects become crucial when the density difference exists in the flow regimes. The Soret effect, for instance, has been utilized for isotope separation. In a mixture between gases with very light molecular weight (He, H_2) and medium molecular weight (N_2, air), the Dufour effect was found to be of considerable magnitude such that it cannot be neglected[3]. The Dufour and Soret effects were studied by many researchers. Kafoussias and Williams[4] studied the thermo-diffusion and diffusion-thermo effects on the mixed free-forced convective and mass transfer of steady laminar boundary layer flow over a vertical flat. Anghel et al.[5] investigated the Dufour and Soret effects on the free convection over a vertical surface embedded in a porous medium. Postelnicu[6] numerically studied the influence of a magnetic field on the heat and mass transfer by the natural convection from the vertical surfaces in a Darcy porous media considering the Soret and Dufour effects. Lakshmi-Narayana and Murthy[7] considered both the Soret and Dufour effects on a free convective boundary layer from a horizontal plate in a Darcy porous medium. Mohamad[8] studied the Soret effect on the unsteady magnetohydrodynamics (MHD) free convetion heat and mass transfer flow past a semi-infinite vertical plate in a Darcy

porous medium in the presence of chemical reaction and heat generation. Afify[9] carried out a numerical analysis to study the free convective heat and mass transfer of an incompressible electrically conducting fluid over a stretching sheet in the presence of suction and injection with the Soret and Dufour effects. Vempati and Laxmi-Narayana-Gari[10] considered the effect of Dufour and Soret effects on the free convection and mass transfer of an unsteady MHD flow over an infinite vertical plate embedded in a Darcy porous medium under the oscillattory suction velocity and the thermal radiation. Shyam et al.[11] examined the Soret and Dufour effects on the MHD natural convection over a vertical surface embedded in a Darcy porous medium in the presence of thermal radiation. Recently, Eugen and Adrian[12] considered the double-diffusive natural convection past a vertical plate embedded in a fluid-saturated porous medium with the significant Soret and Dufour cross-diffusion effects. Cheng[13] numerically investigated the Soret and Dufour effects on the free convection heat and mass flow rate over a vertical cone in a Darcy porous medium.

In recent years, considerable attention has been devoted to study the MHD flows and heat transfer because of the applications in engineering, agriculture, petroleum industries, geophysics, and astrophysics. Kinyanjui et al.[14] studied the transient free convection heat over an impulsively started vertical plate in the presence of thermal radiation. Al-Odat and Al-Azab[15] numerically studied the transient MHD free convective heat and mass transfer over a moving vertical surface in the presence of a homogeneous chemical reaction of first order. Palani and Srikanth[16] studied the MHD flow of an electrically conducting fluid over a semi-infinite vertical plate under the influence of the transversely applied magnetic field. The steady laminar MHD mixed convection heat transfer about a vertical plate was numerically investigated by taking the effect of Ohmic heating and viscous dissipation[17] into account. The combined effects of the mixed convection with chemical reaction and thermal radiation on the MHD flow of an electrically conducting fluid over a vertical surface in the porous media were numerically investigated[18]. Makinde[19] investigated the MHD boundary layer flow with the heat and mass transfer over a moving vertical plate in the presence of magnetic field and convective heat exchange at the surface. Recently, Ali-Chamkha and Mansour[20] examined the effect of chemical reaction, thermal radiation, and heat generation or absorption on the unsteady MHD free convective heat and mass transfer along an infinite vertical plate. More recently, Ramana-Murthy and Hari[21] examined the nature of the various flow entities of an unsteady two-dimensional laminar convective boundary layer flow of a viscous incompressible and chemically reacting fluid along a semi-infinite vertical plate with suction by taking the effects of dissipation into account.

It should be mentioned that the majority of the above studies focused on the steady state conditions using the Darcy model, which only refers to the bulk matrix drag experienced by the fluid because of the linear pressure drop across the porous material. In contrast, the transient coupled heat and mass flow problems in the porous media have received little attention. This is because the transient heat transfer is usually difficult to solve either analytically or numerically. In fact, there is no actual flow situation, which does not involve unsteadiness, and examples of transient convective flows are numerous, including cooling of electronic devices in which the heat generation is not constant but time varying. The Darcy model is valid when the Reynolds number based on the pore size are smaller than unity. For the higher velocity fluids and/or the porous material of the large pore radius, the Darcy model is inadequate since it neglects the porous medium inertial effect, which becomes significant and quadratic drag effect because of inertia dominance over viscous forcers. Inertial effects are taken into consideration in the Darcy-Forchheimer model, which is a modification of the original Darcy law by adding the quadratic inertial term. Murthy and Singh[22] analyzed the Forchheimer free convection heat and mass transfer near a vertical surface embedded in a fluid saturated porous medium by similarity solutions. Jumah-Rami et al.[23] obtained similarity solutions for the Darcy-Forchheimer mixed convection from a vertical flat plate embedded in a fluid-saturated porous medium under the coupled effects of thermal and mass diffusion. Mohamed and Gorla[24] studied the problem of

free convention flow over a horizontal or a vertical flat plate embedded in a fluid-saturated non-Darcy porous medium, considering the Forchheimer extension. Dulal and Mondal[25] presented a numerical investigation of the effect of temperature-dependent viscosity on the non-Darcy MHD mixed convective heat transfer past a porous medium by taking the Ohmic dissipation and the non-uniform heat source/sink into account. Ahmed and Barua[26] analytically investigated the unsteady MHD free convective flow past a vertical porous plate immersed in a porous medium with Hall current, thermal diffusion, and heat source. Partha[27] numerically studied the natural convection in a non-Darcy porous medium by a temperature-concentration-dependent density relation.

In view of the above literature review, the present article is to study the Dufour and Soret effects on a two-dimensional unsteady MHD double-diffusive free convective of an electrically conducting fluid over a heated permeable plate embedded in a non-Darcy porous medium. The governing partial differential equations are solved by an implicit finite difference method of Crank-Nicolson type. The transient behaviors of the velocity, the temperature, the concentration, the skin friction coefficient, the Nusselt number, and the Sherwood number are analyzed for the various parameters entering into the problem under consideration.

2 Problem formulation and mathematical analysis

Consider the unsteady non-Darcy MHD double-diffusive free convective flow of an electrically conducting fluid over an impulsively started isothermal vertical plate embedded in a porous medium. The flow is assumed to be in the x-direction, which is taken along the vertical plate in the upward direction, and the y-axis is normal to the plate. A uniform magnetic field is applied transversely to the fluid flow direction. Initially, it is assumed that the plate and the fluid are at the same constant temperature T_∞ with the concentration level C_∞ at all points. For $t > 0$, the plate starts moving impulsively in the vertical direction with the constant velocity u_0, the temperature is suddenly raised to T_w ($> T_\infty$), and the concentration level at the plate is raised to $C_\mathrm{w}(> C_\infty)$. It is assumed that the fluid properties are constant, except for the influence of the density variation with the temperature, which is considered only in the body force term, both the fluid and solid matrices are in the local thermal equilibrium, the permeability porous medium is constant, and the viscous dissipation and the Joule heating are negligible. The Soret and Dufour effects are taken into consideration. Under these assumptions along with the Boussinesq approximation, the governing equations are given by

$$\frac{\partial u}{\partial x} + \frac{\partial v}{\partial y} = 0, \tag{1}$$

$$\frac{\partial u}{\partial t} + u\frac{\partial u}{\partial x} + v\frac{\partial u}{\partial y} = \nu\frac{\partial^2 u}{\partial y^2} + g\beta_\mathrm{t}(T - T_\infty) + g\beta_\mathrm{c}(C - C_\infty) - \Big(\frac{\nu}{K_\mathrm{p}} + \frac{\sigma {B_0}^2}{\rho}\Big)u - \frac{F}{K_\mathrm{p}}u^2, \tag{2}$$

$$\frac{\partial T}{\partial t} + u\frac{\partial T}{\partial x} + v\frac{\partial T}{\partial y} = \alpha_\mathrm{e}\frac{\partial^2 T}{\partial y^2} + \frac{D_\mathrm{m}K_\mathrm{t}}{c_\mathrm{s}c_p}\frac{\partial^2 C}{\partial y^2}, \tag{3}$$

$$\frac{\partial C}{\partial t} + u\frac{\partial C}{\partial x} + v\frac{\partial C}{\partial y} = D_\mathrm{m}\frac{\partial^2 C}{\partial y^2} + \frac{D_\mathrm{m}K_\mathrm{t}}{T_\mathrm{m}}\frac{\partial^2 T}{\partial y^2}. \tag{4}$$

The initial and boundary conditions for the velocity, temperature, and concentration fields are given by

$$\begin{cases} u = u_\mathrm{p}, \quad v = 0, \quad T = T_\infty, \quad C = C_\infty \quad \text{for} \ \ t \leqslant 0, \ \ y \geqslant 0, \\ u = u_0, \quad v = 0, \quad T = T_\mathrm{w}, \quad C = C_\mathrm{w} \quad \text{for} \ \ t > 0 \ \ \text{at} \ \ y = 0, \\ u = u_0, \quad v = 0, \quad T = T_\infty, \quad C = C_\infty \quad \text{for} \ \ t > 0 \ \ \text{as} \ \ y \to \infty, \\ u = 0, \quad v = 0, \quad T = T_\infty, \quad C = C_\infty \quad \text{for} \ \ t > 0 \ \ \text{at} \ \ x = 0, \end{cases} \tag{5}$$

where x and y are the dimensional distances along and normal to the plate, respectively, u and v are the average velocity components along the x- and y-directions, respectively, t is the time, T is the temperature, C is the concentration, β_{t} and β_{c} are the thermal and concentration expansion coefficients, respectively, ν is the effective kinematic viscosity, α_{e} is the effective thermal diffusivity, F is the dimensional Forchheimer coefficient, K_{p} is the permeability of the medium, D_{m} is the coefficient of mass diffusivity, T_{m} is the mean fluid temperature, K_{t} is the thermal diffusion ratio, c_p is the specific heat at constant pressure, and c_{s} is the concentration susceptibility.

To write the non-dimensional form of the governing equations, the following dimensionless quantities are introduced:

$$\begin{cases} X = \dfrac{xu_0}{\nu}, \quad Y = \dfrac{yu_0}{\nu}, \quad \tau = \dfrac{u_0^2 t}{\nu}, \quad U = \dfrac{u}{u_0}, \quad V = \dfrac{v}{u_0}, \\ \theta = \dfrac{T - T_\infty}{T_{\mathrm{w}} - T_\infty}, \quad \phi = \dfrac{C - C_\infty}{C_{\mathrm{w}} - C_\infty}, \quad M = \dfrac{\sigma B_0^2 \nu}{\rho u_0^2}, \quad Da = \dfrac{u_0}{\nu} K_{\mathrm{p}}, \\ \Gamma = \dfrac{F\nu}{K_{\mathrm{p}} u_0}, \quad Gr_{\mathrm{t}} = \dfrac{\nu g \beta_{\mathrm{t}} (T_{\mathrm{w}} - T_\infty)}{u_0^3}, \quad Gr_{\mathrm{c}} = \dfrac{\nu g \beta_{\mathrm{c}} (C - C_\infty)}{u_0^3}, \\ Du = \dfrac{D_{\mathrm{m}} K_{\mathrm{t}} (C_{\mathrm{w}} - C_\infty)}{c_{\mathrm{s}} c_p \nu (T_{\mathrm{w}} - T_\infty)}, \quad Sr = \dfrac{D_{\mathrm{m}} K_{\mathrm{t}} (T_{\mathrm{w}} - T_\infty)}{\nu T_{\mathrm{m}} (C_{\mathrm{w}} - C_\infty)}, \\ Pr = \dfrac{\nu}{\alpha_{\mathrm{e}}}, \quad Sc = \dfrac{\nu}{D_{\mathrm{m}}}, \quad U_{\mathrm{p}} = \dfrac{u_{\mathrm{p}}}{u_0}. \end{cases} \tag{6}$$

Therefore, using the above dimensionless quantities, the governing equations (1)–(4) are reduced to the following non-dimensional form:

$$\frac{\partial U}{\partial X} + \frac{\partial V}{\partial Y} = 0, \tag{7}$$

$$\frac{\partial U}{\partial \tau} + U\frac{\partial U}{\partial X} + V\frac{\partial U}{\partial Y} = \frac{\partial^2 U}{\partial Y^2} + Gr_{\mathrm{t}}\theta + Gr_{\mathrm{c}}\phi - \Big(\frac{1}{Da} + M\Big)U - \Gamma U^2, \tag{8}$$

$$\frac{\partial \theta}{\partial \tau} + U\frac{\partial \theta}{\partial X} + V\frac{\partial \theta}{\partial Y} = \frac{1}{Pr}\frac{\partial^2 \theta}{\partial Y^2} + Du\frac{\partial^2 \phi}{\partial Y^2}, \tag{9}$$

$$\frac{\partial \phi}{\partial \tau} + U\frac{\partial \phi}{\partial X} + V\frac{\partial \phi}{\partial Y} = \frac{1}{Sc}\frac{\partial^2 \phi}{\partial Y^2} + Sr\frac{\partial^2 \theta}{\partial Y^2}, \tag{10}$$

and the corresponding initial and boundary conditions in the dimensionless form can be written as

$$\begin{cases} U = 1, \quad V = 0, \quad \theta = 0, \quad \phi = 0 \quad \text{for } \tau \leqslant 0,\ Y \geqslant 0, \\ U = U_{\mathrm{p}}, \quad V = 0, \quad \theta = 1, \quad \phi = 1 \quad \text{for } \tau > 0 \text{ at } Y = 0, \\ U = 1, \quad V = 0, \quad \theta = 0, \quad \phi = 0 \quad \text{for } \tau > 0 \text{ as } Y \to \infty, \\ U = 0, \quad V = 0, \quad \theta = 0, \quad \phi = 0 \quad \text{for } \tau > 0 \text{ at } X = 0, \end{cases} \tag{11}$$

where τ is the dimensionless time, Gr_{t} and Gr_{c} are the thermal Grashof number and the modified solutal Grashof number, respectively, Da is the Darcy number, Γ is the Forchheimer parameter, M is the magnetic field parameter, Du is the Dufour number, Sr is the Soret number, Pr is the Prandtl number, and Sc is the Schmidt number.

With the velocity, temperature, and concentration fields, it is customary to study the skin friction coefficient and the rate of heat and mass transfer. Given the velocity field in the boundary layer, the skin friction coefficient can be written as follows:

$$C_{\mathrm{f}} = \frac{1}{\rho u_0^2}\Big(\mu\frac{\partial u}{\partial y}\Big)_{y=0} = \Big(\frac{\partial U}{\partial Y}\Big)_{Y=0}. \tag{12}$$

With the temperature field, the rate of heat transfer coefficient can be obtained in the following term of the Nusselt number:

$$Nu = \frac{q_{\mathrm{w}}\nu}{k_{\mathrm{e}}u_0(T_{\mathrm{w}} - T_\infty)} = -\Big(\frac{\partial\theta}{\partial Y}\Big)_{Y=0}, \tag{13}$$

where

$$q_{\mathrm{w}} = -k_{\mathrm{e}}\Big(\frac{\partial T}{\partial y}\Big)_{y=0}.$$

With the concentration field, the rate of mass transfer coefficient can be computed in the term of the Sherwood number as

$$Sh = \frac{C_{\mathrm{w}}\nu}{D_{\mathrm{m}}u_0(C_{\mathrm{w}} - C_\infty)} = -\Big(\frac{\partial\phi}{\partial Y}\Big)_{Y=0}, \tag{14}$$

where

$$C_{\mathrm{w}} = -D_{\mathrm{m}}\Big(\frac{\partial C}{\partial y}\Big)_{y=0}.$$

3 Numerical solution

The unsteady, non-linear, and coupled partial differential equations (7)–(10) together with the boundary and initial conditions (11) are numerically solved by an implicit finite-difference technique of the Cranck-Nicolson type. All the first-order derivatives with respect to time terms are computed by the following central finite formula:

$$\frac{\partial\psi}{\partial\tau} = \frac{\psi_{i,j}^{n+1} - \psi_{i,j}^{n}}{\Delta\tau}, \tag{15}$$

where ψ stands for U, V, θ, and ϕ, n refers to the time, and i and j refer to the space coordinates. All the second-order derivatives with respect to X are computed by the following central finite formula:

$$\frac{\partial\psi}{\partial\tau} = \frac{\psi_{i+1,j}^{n+1} - \psi_{i+1,j}^{n} - \psi_{i,j}^{n+1} - \psi_{i,j}^{n} + \psi_{i-1,j}^{n+1} - \psi_{i-1,j}^{n}}{2(\Delta X)^2}. \tag{16}$$

Besides, all the second-order derivatives with respect to Y are computed by the following central finite formula:

$$\frac{\partial\psi}{\partial\tau} = \frac{\psi_{i,j+1}^{n+1} - \psi_{i,j+1}^{n} - \psi_{i,j}^{n+1} - \psi_{i,j}^{n} + \psi_{i,j-1}^{n+1} - \psi_{i,j-1}^{n}}{2(\Delta Y)^2}. \tag{17}$$

With the above central finite difference approximation, the governing equations are transformed into a tridiagonal system, and the system can be solved by the tridiagonal technique.

The computational domain is considered as a rectangle with the width of 1 ($X_{\max}$) and the length of 8 ($Y_{\max}$), where $Y_{\max}$ corresponds to $Y = \infty$, which lies very well outside the momentum, thermal, and concentration boundary layers. The maximum value of Y is chosen after some preliminary investigations so that the boundary conditions are satisfied with the tolerance of 10^{-6}. A grid independence study is carried out with different values of mesh sizes. After experimenting with a few set of mesh sizes, the mesh sizes are fixed at $\Delta X = 0.01$ and $\Delta Y = 0.01$ with the time step $\Delta\tau = 0.005$. The mesh sizes are reduced by 50% in one direction and then in both directions, and the results are compared. It is found that, when the mesh size is reduced by 50% in the X-direction or both the X- and the Y-directions, the results remain

the same. Thus, because of computational cost and accuracy considerations, the above mesh size is considered as an optimum for the present computations.

The iteration error ε, in the percentage form, is defined as follows:

$$\varepsilon = \left| \frac{\psi_{i,j}^{n+1} - \psi_{i,j}^{n}}{\psi_{i,j}^{n}} \right| \times 100\%. \tag{18}$$

The value of tolerance ε is chosen as 10^{-6}.

An examination of data for the unsteady solution revealed little or no change in U, V, θ, and ϕ after $\tau = 6$ for all computations. Thus, the result for $\tau = 6$ is taken essentially as the steady state values.

To verify the accuracy of the present computer code, particular results are compared with those available in the literature. The unsteady results without the Soret and Dufour effects are compared with those in Ref. [16]. Figure 1 displays this comparison. It can be seen that the agreement between the results is excellent. This has established confidence in the numerical results to be reported in this article.

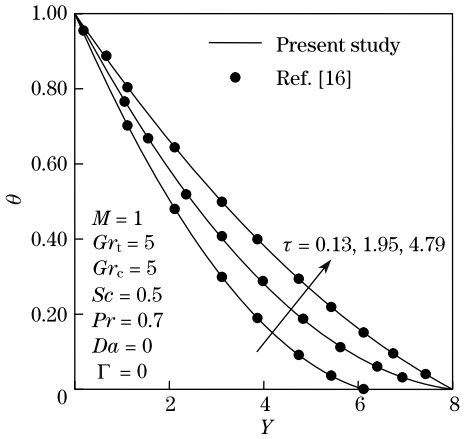

Fig. 1 Comparison of transient dimensionless temperature distributions of present study and those in Ref. [16]

4 Results and Discussion

A parametric study is carried out to investigate the effects of all parameters involved on the transient velocity, temperature, concentration profiles and the transient skin friction coefficient, the Nusselt number, and the Sherwood number.

Figure 2 shows the effect of the Dufour number on the transient velocity, temperature, and concentration profiles. The Dufour number denotes the contribution of the concentration gradients to the thermal energy flux in the flow. It can be seen that an increase in the Dufour number causes a rise in the velocity and temperature and a drop in the concentration. In addition, the velocity, the temperature, and the concentration increase when the time elapses, and the thermal and concentration boundary layers increase with time.

Figure 3 illustrates the influence of the Dufour number on the time evolution of the velocity, the temperature, and the concentration at $Y = 4$. It is clear that all the three quantities increase exponentially with time until they reach the steady state values. It is revealed that the time required to reach the steady state for the temperature is longer as comparison with the velocity and the concentration. Moreover, the velocity and the temperature increase with the Dufour number, while the concentration decreases. The thickness of the temperature boundary

layer and the thickness of the concentration boundary layer decrease when the Dufour number increases.

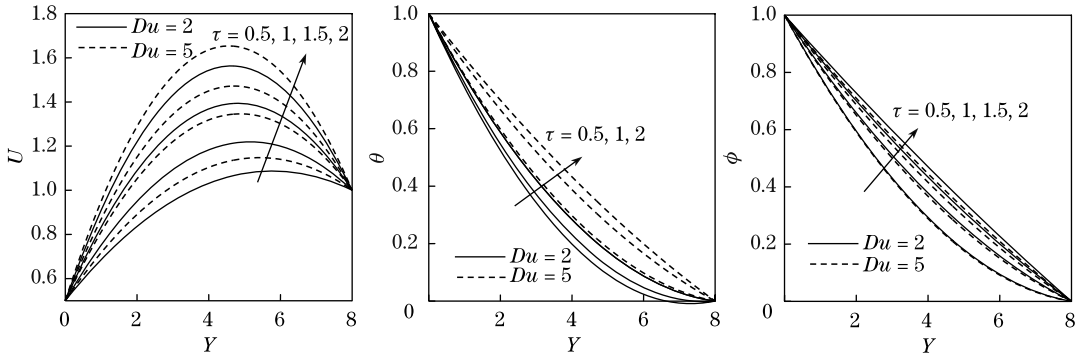

(a) Transient velocity distributions (b) Transient temperature distributions (c) Transient concentration distributions

Fig. 2 Effects of Du on transient velocity distributions, transient temperature distributions, and transient concentration distributions for $Sr = 1$, $Da = 2$, $\Gamma = 1.25$, $M = 1$, $Gr_{\mathrm{t}} = 5$, $Gr_{\mathrm{c}} = 5$, $Sc = 0.22$, $Pr = 0.7$, and $U_{\mathrm{p}} = 0.5$

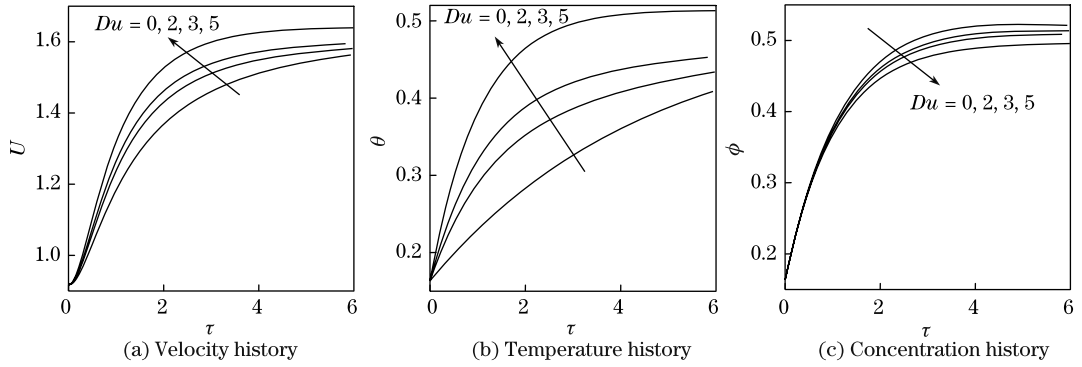

(a) Velocity history (b) Temperature history (c) Concentration history

Fig. 3 Effects of Du on velocity history, temperature history, and concentration history at $Y = 4$ for $Sr = 1$, $Da = 2$, $\Gamma = 1.25$, $M = 1$, $Gr_{\mathrm{t}} = 5$, $Gr_{\mathrm{c}} = 5$, $Sc = 0.22$, $Pr = 0.7$, and $U_{\mathrm{p}} = 0.5$

Figure 4 depicts the time variation of the skin friction, the Nusselt number, and the Sherwood number at different values of the Dufour number. It can be noticed that the local Nusselt number decreases for the larger Dufour number. In contrast, the Sherwood number increases for the larger Dufour number.

Figure 5 shows the effect of the Soret number on the transient velocity, temperature, and concentration profiles. The Soret number describes the effect of temperature gradients inducing imperative mass diffusion effects. It can be seen that an increase in the Soret number causes a rise in the velocity and the concentration and a drop in the temperature within the boundary layer. In addition, the velocity, the temperature, and the concentration increase when the time elapses.

Figure 6 illustrates the influence of the Soret number on the time evolution of the velocity, the temperature, and the concentration at $Y = 4$. It is clear that all flow variables increase exponentially with time until they reach the steady state values. The time required to reach the steady state for the temperature is longer compared to the velocity and the concentration. Moreover, the velocity and the temperature increase with the Soret number, while the concentration decreases.

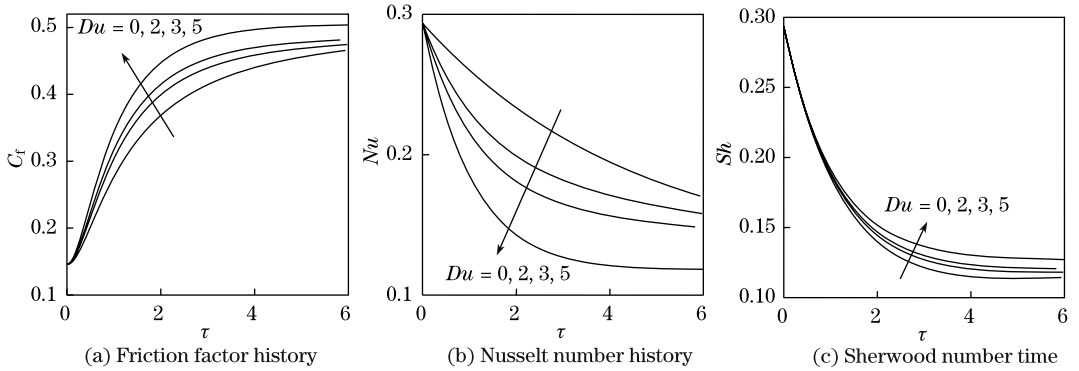

(a) Friction factor history (b) Nusselt number history (c) Sherwood number time evolution

Fig. 4 Effects of Du on friction factor history, Nusselt number history, and Sherwood number time evolution at $Y = 4$ for $Sr = 1$, $Da = 2$, $\Gamma = 1.25$, $M = 1$, $Gr_t = 5$, $Gr_c = 5$, $Sc = 0.22$, $Pr = 0.7$, and $U_p = 0.5$

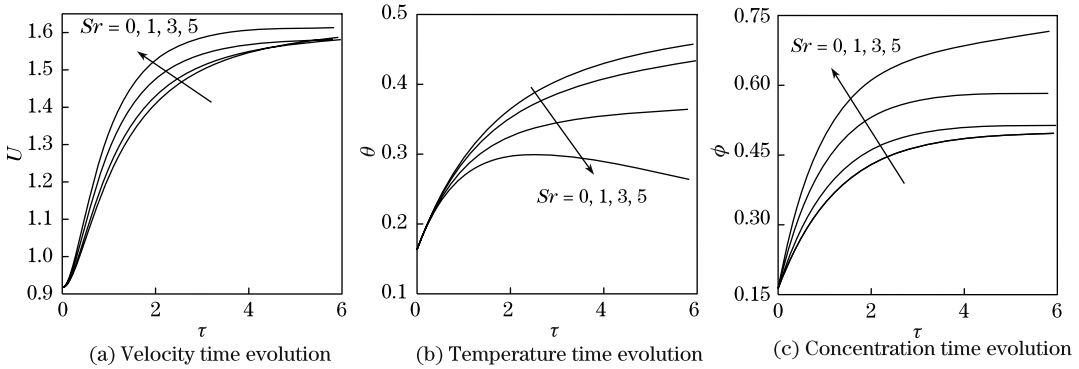

(a) Velocity time evolution (b) Temperature time evolution (c) Concentration time evolution

Fig. 5 Effects of Sr on velocity time evolution, temperature time evolution, and concentration time evolution at $Y = 4$ for $Du = 2$, $Da = 2$, $\Gamma = 1.25$, $M = 1$, $Gr_t = 5$, $Gr_c = 5$, $Sc = 0.22$, $Pr = 0.7$, and $U_p = 0.5$

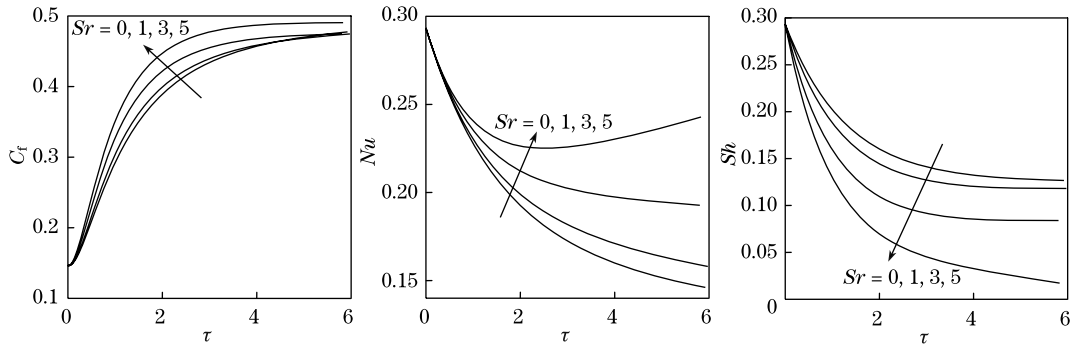

(a) Skin friction time evolution (b) Nusselt number time evolution (c) Sherwood number time evolution

Fig. 6 Effects of Sr on skin friction time evolution, Nusselt number time evolution, and Sherwood number time evolution at $Y = 4$ for $Du = 2$, $Da = 2$, $\Gamma = 1.25$, $M = 1$, $Gr_t = 5$, $Gr_c = 5$, $Sc = 0.22$, $Pr = 0.7$, and $U_p = 0.5$

Figure 7 depicts the time variation of the skin friction, the Nusselt number, and the Sherwood number at different values of the Soret number. It can be noticed that the local Nusselt number decreases with the larger Soret number. In contrast, the Sherwood number increases with larger values of the Soret number. The smaller Soret number and the larger Dufour number coincide with the decreasing temperature difference accompanied with the increasing concentration difference. Therefore, the wall temperature gradient is reduced. The previous figures demonstrate that, as the Soret number decreases and the Dufour number increases, the heat transfer rate is weakened. However, the shear stress and the mass transfer rate are improved. This is because the smaller Sr and the larger Du accompany the stronger diffusion-thermo and weaker thermo-diffusion effects.

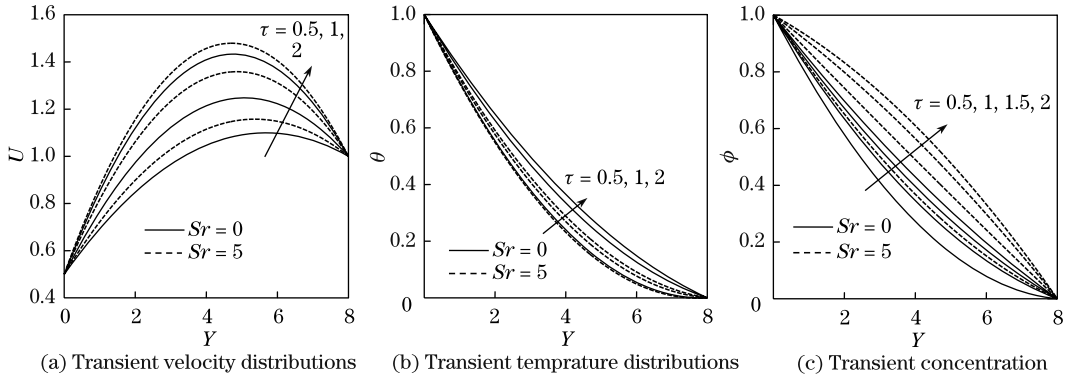

(a) Transient velocity distributions (b) Transient temprature distributions (c) Transient concentration distributions

Fig. 7 Effects of Sr on transient velocity distributions, transient temprature distributions, and transient concentration distributions for $Du = 2$, $Da = 2$, $\Gamma = 1.25$, $M = 1$, $Gr_t = 5$, $Gr_c = 5$, $Sc = 0.22$, $Pr = 0.7$, and $U_p = 0.5$

The effects of magnetic parameter on the velocity time variation and the transient distributions are plotted in Fig. 8. It is clear that the hydrodynamics boundary layers become thicken gradually with time. The presence of the magnetic field produces a resistive force that decelerates the fluid flow in the porous medium and increases the boundary layer thicknesses.

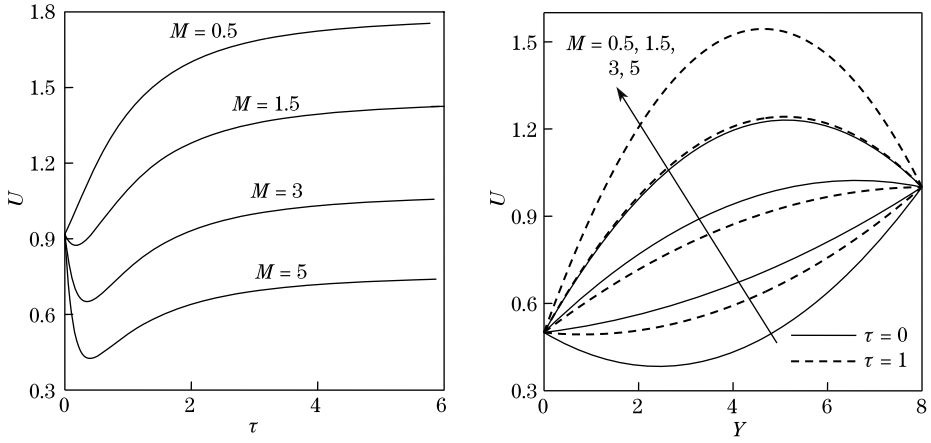

(a) Velocity variation with time (b) Velocity distributions

Fig. 8 Effect of M on velocity variation with time at $Y = 4$ and velocity distributions for $Gr_t = 5$, $Gr_c = 5$, $Sc = 0.22$, $Pr = 0.7$, $U_p = 0.5$, $Du = 2$, $Da = 2$, $\Gamma = 1.25$, and $Sr = 1$

Figure 9 illustrates the influence of magnetic parameter on the time variation of the skin friction coefficient. It can be seen that the the skin friction coefficient decreases dramatically as the magnetic parameter increases.

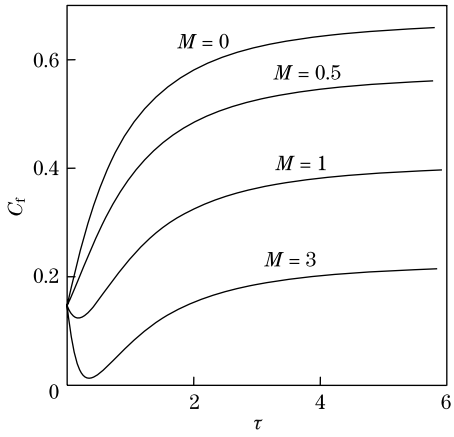

Fig. 9 Skin friction coefficient with time variation for different values of M at $Y = 4$ for $Gr_t = 5$, $Gr_c = 5$, $Sc = 0.22$, $Pr = 0.7$, $U_p = 0.5$, $Du = 2$, $Sr = 1$, $Da = 2$, and $\Gamma = 1.25$

The influences of permeability parameter Da on the velocity time evolution and the transient velocity profiles are displayed in Fig. 10. The velocity increases significantly with the increase in the permeability parameter. For the large Darcy number, the porosity on the media increases. Hence, the fluid flows quickly.

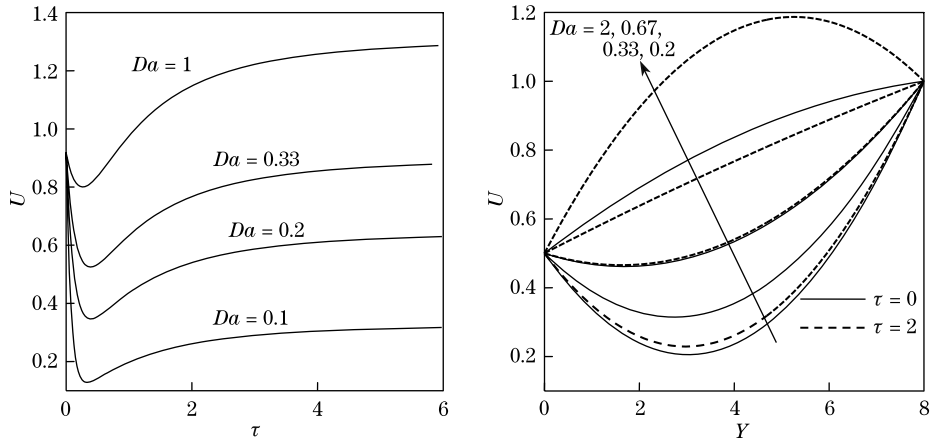

(a) Velocity variation with time at $Y = 4$ (b) velocity distribution for different values of Da

Fig. 10 Effect of Da on velocity variation with time at $Y = 4$ and velocity distribution for $Gr_t = 5$, $Gr_c = 5$, $Sc = 0.22$, $Pr = 0.7$, $U_p = 0.5$, $Du = 2$, $Sr = 1$, $M = 1.5$, and $\Gamma = 1.25$

Figure 11 shows the effect of the Forchheimer parameter Γ on the transient velocity profiles. The case $\Gamma = 0$ corresponds to a purely Darcy porous media. An increase in the Forchheimer parameter (which increases the quadratic drag in Eq. (8)) is seen to dramatically lower the velocity profiles.

The effect of the thermal Grashof number on the transient velocity profiles is plotted in Fig. 12. It can be seen that the velocity increases substantially as the thermal Grashof number increases. The lowest velocity value corresponds to the case $Gr_t = 0$, i.e., the forced convection.

The maximum velocity occurs at $Y = 4$ for all profiles. The thermal Grashof number embodies the relative significance of the thermal bouyancy forces to the viscous hydrodynamic force. Higher Gr_t values mean stronger convective currents which therefore enhance the flow velocities.

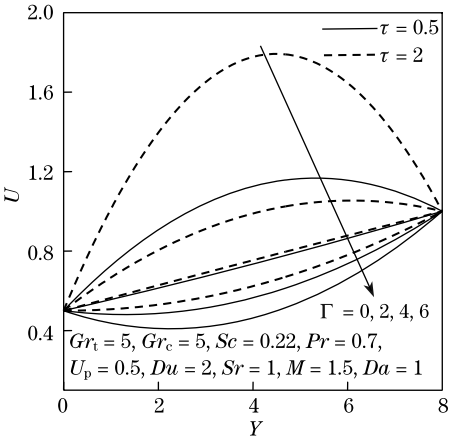

Fig. 11 Effects of Γ on transient velocity profiles

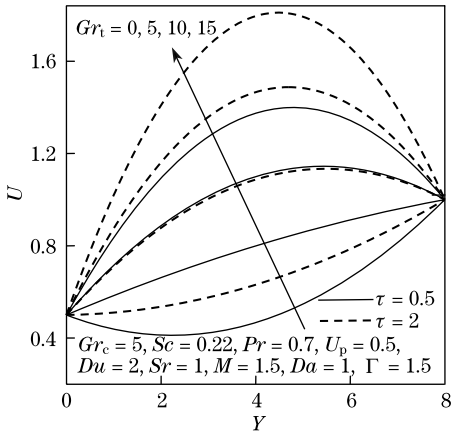

Fig. 12 Effects of Gr_t on transient velocity profiles

The influences of the solutal Grashof number Gr_c on the transient velocity distributions in the boundary layer are illustrated in Fig. 13. The solutal Grashof number is defined as the ratio of the species bouyancy force to the viscous hydrodynamic force. The velocity profile attains a distinctive maximum value in the vicinity of vertical plate and then decreases to reach the free stream value. For $Gr_c = 0$, i.e., the forced convection mass transfer, there is a completely different behavior of the velocity profile. In such way, the velocity decreases at first, and the profile attains a distinct minimum value and then increases. Moreover, the concentration boundary layer grows up when the time elapses.

The transient temperature profiles at different Prandtl numbers are illustrated in Fig. 14. The values of the Prandtl number are chosen for air ($Pr = 0.71$), electrolytic solution ($Pr = 1$), water ($Pr = 7$), and water at 4 °C ($Pr = 11.4$). It can be noticed that an increase in the Prandtl number results in a decrease in the temperature profiles and more uniform temperature distribution across the boundary layer. This is because that the Prandtl number increases by either increase of the kinematic viscosity or decrease of the thermal conductivity of the porous media. The smaller values of Pr correspond to the increase in the effective thermal conductivity of pours media. Hence, heat is able to diffuse away from the heated surface more promptly. The heat transfer rate in the term of the Nusselt number is improved for larger values of Pr, as shown in Fig. 15. Furthermore, the Nusselt number increases when the time elapses, and more time is required to reach the steady state heat transfer rate for the larger values of Pr.

The effects of the Schmidt number Sc on the concentration time variation and on the transient concentration profiles are plotted in Fig. 16. The Schmidt number represents the ratio of the momentum to the mass diffusivity. The values of Sc are selected for the gases representing diffusing chemical species of most common interest in air, namely, hydrogen ($Sc = 0.22$), water vapor ($Sc = 0.6$), oxygen ($Sc = 0.66$), methanol ($Sc = 1$), and propyl-benzene ($Sc = 2.62$) at 20 °C and one atmospheric pressure. It can be seen that the concentration profile is linear for the hydrogen and falls quickly for methanol and propyl-benzene compared to the water vapor. In addition, the concentration increases when Sc decreases, since the larger values of Sc are equivalent to the decrease in the chemical molecular diffusivity.

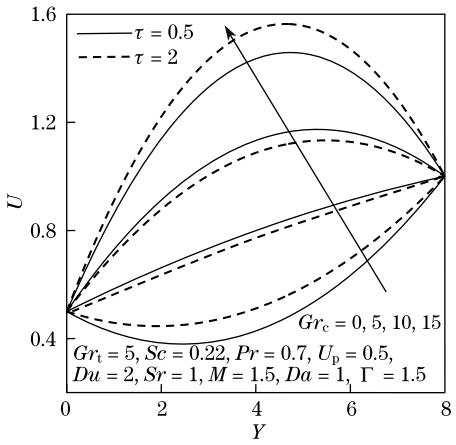

Fig. 13 Effect of Gr_c on transient velocity profiles

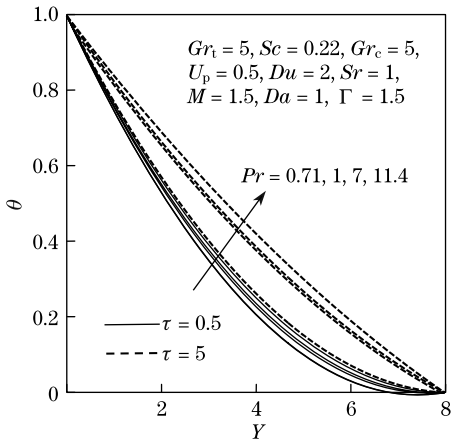

Fig. 14 Effect of Pr on transient temperature profiles

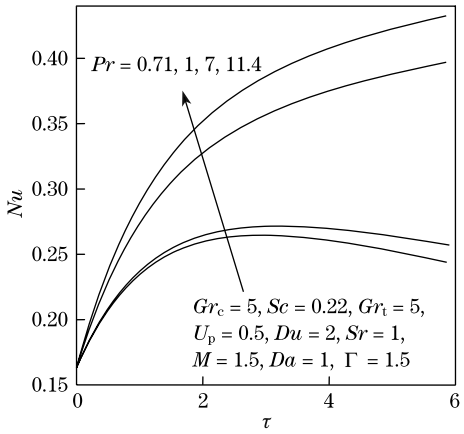

Fig. 15 Influence of Pr on Nu variation with time at $Y = 4$

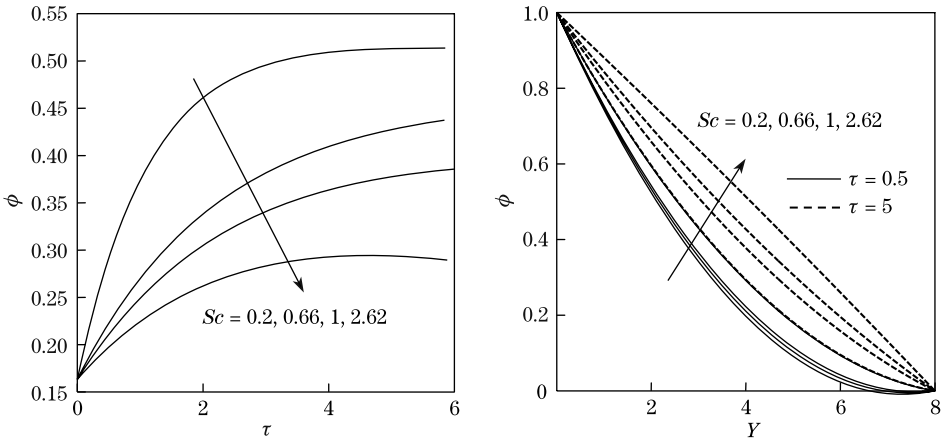

(a) Concentration variation with time at $Y = 4$ (b) Transient concentration profiles

Fig. 16 Effect of Sc on concentration variation with time at $Y = 4$ and transient concentration profiles for $Gr_c = 5$, $Sc = 0.22$, $Gr_t = 5$, $U_p = 0.5$, $Du = 2$, $Sr = 1$, $M = 1.5$, $Da = 1$, and $\Gamma = 1.5$

Figure 17 demonstrates the influence of the Schmidt number Sc on mass transfer rate in terms of the Sherwood number. It can be seen that the mass transfer rate is enhanced by the increase in the Schmidt number.

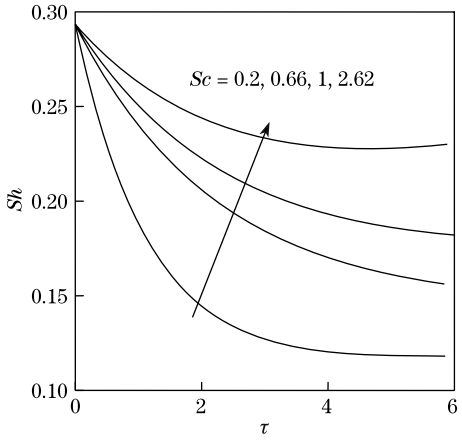

Fig. 17 Effect of Sc on Sh variation with time at $Y = 4$ for $Gr_c = 5$, $Sc = 0.22$, $Gr_t = 5$, $U_p = 0.5$, $Du = 2$, $Sr = 1$, $M = 1.5$, $Da = 1$, and $\Gamma = 1.5$

5 Conclusions

The finite difference investigation is carried out for the unsteady MHD double-diffusive of an electrically conducting fluid over a flat plate embedded in a non-Darcy porous medium taking the Dufour and Soret effects into account. The dimensionless governing equations are solved by a finite difference method of the Cranck-Nicolson type. The present numerical results are compared with the previously reported data, and the agreement is excellent. The transient velocity, temperature, and the concentration values increase when the time elapses until they reach the steady state values. It is found that the temperature profiles increase with the decrease in the Soret number, whereas the concentration profiles decrease with the increase in the Dufour number. Moreover, it is observed that the skin friction coefficient and the Nusselt number increase when the Dufour number decreases or the Soret Number increases. Whereas, the Sherwood number decreases with the increase in the Soret number and the decrease in the Dufour number. The results of this work show that the Dufour and Soret numbers have a significant effect on the velocity, the temperature, and the concentration variation with time and position. Thus, these effects should be considered when the double-diffusive phenomena are studied. Finally, both the heat and mass transfer rates tend to decrease when the time elapses, while the skin friction coefficient increases with time.

References

[1] Nield, D. A. and Bejan, A. *Convection in Porous Media,* 3rd ed., Springer, New York (2006)

[2] Ingham, D. and Pop, I. *Transport Phenomena in Porous Media* III, Elsevier, Oxford (2005)

[3] Eckert, E. R. G. and Drak, R. M. *Analysis of Heat and Mass Transfer*, McGraw-Hill, New York (1972)

[4] Kafoussias, N. G. and Williams, E. W. Thermal-diffusion and diffusion-thermo effects on mixed free-forced convective and mass transfer boundary layer flow with temperature dependent viscosity. *International Journal of Engineering Science*, **33**(9), 1369–1384 (1995)

[5] Anghel, M., Takhar, H. S., and Pop, I. Dufour and Soret effects on free convection boundary layer over a vertical surface embedded in a porous medium. *Studia Universitatis Babes-Bolyai, Mathematica*, **45**, 11–21 (2000)

[6] Postelnicu, A. Influence of a magnetic field on heat and mass transfer by natural convection from vertical surfaces in porous media considering Soret and Dufour effects. *International Journal of Heat and Mass Transfer*, **47**(6-7), 1467–1472 (2004)

[7] Lakshmi-Narayana, P. A. and Murthy, P. V. S. N. Soret and Dufour effects on free convection heat and mass transfer from a horizontal flat plate in a Darcy porous medium. *Journal of Heat Transfer*, **130**(10), 104504 (2008)

[8] Mohamad, R. A. Double-diffusive convection-radiation interaction on unsteady MHD flow over a vertical moving porous plate with heat generation and Soret effect. *Applied Mathematical Sciences*, **3**(13), 629–651 (2009)

[9] Afify, A. A. Similarity solution in MHD: effects of thermal-diffusion and diffusion-thermo on free convective heat and mass transfer over a stretching surface considering suction or injection. *Communications in Nonlinear Science and Numerical Simulation*, **14**(5), 2202–2214 (2009)

[10] Vempati, S. R. and Laxmi-Narayana-Gari, A. B. Soret and Dufour effects on unsteady MHD flow past an infinite vertical porous plate with thermal radiation. *Applied Mathematics and Mechanics* (*English Edition*), **31**(12), 1481–1496 (2010) DOI 10.1007/s10483-010-1378-9

[11] Shyam, S. T., Rajeev, M., Rohit, K. G., and Aiyub, K. MHD free convection-radiation interaction along a vertical surface embedded in Darcian porous medium in presence of Soret and Dufour's effects. *Thermal Science*, **14**(1), 137–145 (2010)

[12] Eugen, M. and Adrian, P. Double-diffusive natural convection flows with thermosolutal symmetry in porous media in the presence of the Soret-Dufour effects. *Transport in Porous Media*, **88**(1), 149–167 (2011)

[13] Cheng, C. Y. Soret and Dufour effects on natural convection boundary layer flow over a vertical cone in a porous medium with constant wall heat and mass fluxes. *International Communications in Heat and Mass Transfer*, **38**(1), 44–48 (2011)

[14] Kinyanjui, M., Wanza, J. K. K., and Uppal, S. M. Magnetohydrodynamic free convection heat and mass transfer of a heat generating fluid past an impulsively started infinite vertical porous plate with Hall current and radiation absorption. *Energy Conversion and Management*, **42**(2), 917–931 (2001)

[15] Al-Odat, M. Q. and Al-Azab, T. A. Influence of chemical reaction on transient MHD free convection over a moving vertical plate. *Emirates Journal for Engineering Research*, **12**(3), 15–21 (2007)

[16] Palani, G. and Srikanth, U. MHD flow past a semi-infinite vertical plate with mass transfer. *Nonlinear Analysis*: *Modelling and Control*, **14**(3), 345–356 (2009)

[17] Orhan, A. and Ahmet, K. MHD mixed convection of a viscous dissipating fluid about a permeable vertical flat plate. *Applied Mathematical Modelling*, **33**(11), 4086–4096 (2009)

[18] Dulal, P. and Hiranmoy, M. The influence of thermal radiation on hydromagnetic Darcy-Forchheimer mixed convection flow past a stretching sheet embedded in a porous medium. *Meccanica*, **44**(4), 739–753 (2011)

[19] Makinde, O. D. On MHD heat and mass transfer over a moving vertical plate with a convective surface boundary condition. *The Canadian Journal of Chemical Engineering*, **88**(6), 983–990 (2010)

[20] Ali-Chamkha, M. A. and Mansour, A. A. Unsteady MHD free convective heat and mass transfer from a vertical porous plate with Hall current, thermal radiation and chemical reaction effects. *International Journal for Numerical Methods in Fluids*, **65**(4), 432–447 (2011)

[21] Ramana-Murthy, C. V. and Hari, P. P. Flow past a semi infinite moving vertical plate with viscous dissipation under the influence of magnetic field. *Advances in Theoretical and Applied Mathematics*, **6**(1), 73–87 (2011)

[22] Murthy, P. V. S. N. and Singh, P. Heat and mass transfer by natural convection in a non-Darcy porous medium. *Acta Mechanica*, **138**, 243–254 (1999)

[23] Jumah-Rami, Y., Fawzi, A., and Abu-Al-Rub, F. Darcy-Forchheimer mixed convection heat and mass transfer in fluid saturated porous media. *International Journal of Numerical Methods for Heat and Fluid Flow*, **11**(6), 600–618 (2001)

[24] Mohamed, F. E. and Gorla, R. S. R. Non-Darcy, free convective heat transfer from a plate in a porous medium. *International Journal of Fluid Mechanics Research*, **32**(1), 21–38 (2005)

[25] Dulal, P. and Mondal, H. Effect of variable viscosity on MHD non-Darcy mixed convective heat transfer over a stretching sheet embedded in a porous medium with non-uniform heat source/sink. *Communications in Nonliear Science and Numerical Simulation,* **50**(6), 1553–1565 (2010)

[26] Ahmed, N. K. and Barua, H. D. P. Unsteady MHD free convective flow past a vertical porous plate immersed in a porous medium with Hall current, thermal diffusion and heat source. *International Journal of Engineering, Science and Technology,* **2**(6), 59–74 (2010)

[27] Partha, M. K. Nonlinear convection in a non-Darcy porous medium. *Applied Mathematics and Mechanics* (*English Edition*), **31**(5), 565–574 (2010) DOI 10.1007/s10483-010-0504-6